Nuclear Instruments and Methods in Physics Research B 119 (1996) 137–142

ELSEVIER

NIM B
Beam Interactions with Materials & Atoms

Coherent creation of electron–positron pairs in bound state by high energy photons and charged particles in a crystal

Yu.P. Kunashenko, Yu.L. Pivovarov

Nuclear Physics Institute, P.O. Box 25, 634050 Tomsk, Russia

Received 10 November 1995; revised form received 14 May 1996

Abstract

New brilliant coherent effects arise for e^+e^- pair creation by high energy photons in a crystal, when e^+ and e^- form the neutral bound state (positronium atom moving with relativistic velocity), and for e^+e^- pair creation by relativistic heavy particles passing through the crystal, when e^- (e^+) is captured into the K-shell of the projectile particles.

1. Introduction

New coherent effects occur for the e^+e^- pair creation in a crystal by high energy photon or heavy relativistic particles (nuclei). In the first case, this effect arises when e^+ and e^- form the neutral bound state (positronium atom moving with relativistic velocity – relativistic positronium), and in the second case this effect occurs when created e^- (e^+) is captured into the K-shell of heavy relativistic positive (negative) charged particles.

For the first case, we discuss briefly the results of calculations of type-B coherent photoproduction of relativistic positronium, first considered in [1,2] and show that the cross-section exhibits strong coherent peaks at definite photon energies, with relation of the peak height to background of order of 10^2.

For the second case (pair creation by charged particles), we present the results of calculations of e^+e^- production by relativistic heavy ions (RHI) channeled in a crystal, first suggested in [3]. The channeling allows to avoid the central nucleus–nucleus collisions and study electromagnetic processes at high energies. In the frame of the virtual photon (VP) method, we analyze the coherent effects using calculated cross-section of pair photoproduction in the Coulomb field, and the calculated VP spectrum affecting the RHI during penetration through the crystal. Due to the specific shape of pair photoproduction cross-section with e^- capture into K-shell, and sharply peaked VP spectrum in a crystal, there appears very specific behaviour both of the total and differential over emitted positron energy and angle cross-sections.

2. Coherent photoproduction of relativistic positronium

2.1. Photoproduction of relativistic positronium in an amorphous target

Production of a relativistic positronium (A_{2e}) (positronium atom traveling with relativistic speed) by the photon in the Coulomb field was considered first in Refs. [4,5] and it was shown that the photon can create in the Coulomb field of an atom only the para-positronium (singlet state). According to Refs. [4,5], the cross-section of relativistic positronium photoproduction is connected with the cross-section of e^+e^- photoproduction with parallel momenta of electron and positron, and can be written in the form:

$$\frac{d\sigma_1(A_{2e})}{d\Omega} = \frac{Z^2\alpha^2\beta^3}{8\gamma^4 m^2}\{\sin^2\vartheta\}\Big/\Big\{\Big[1+\beta^2-2\beta\cos\vartheta + (1/2\gamma R_0 m)^2\Big]^2(1-\beta\cos\vartheta)^2\Big\}$$

if the screened Coulomb potential of the target $V(r) = (Ze/r)\exp(-r/R)$ is used, where R is the atomic screening radius and Z is the charge of the target nucleus. Here, $\gamma_{A_{2e}} = \omega/(2m-\varepsilon_0) \simeq \omega/2m$ is the Lorentz factor or relativistic factor and β is the velocity of created A_{2e}, α is the fine structure constant, and ε_0 is the binding energy of positronium.

PII S0168-583X(96)00345-X

2.2. Coherent photoproduction of relativistic positronium in a crystal

Let a photon enter a crystal parallel to the crystallographic axis (along OZ direction). We shall consider the interaction with a single axis (a string consisting of N atoms), i.e. the coherent process of type B. Describing the incident photons and motion of created positronium atom as a whole by the plane waves and consider the potential of the atomic string as the perturbation, similar to Section 2.1 the cross section of A_{2e} photoproduction in a crystal is obtained by summing of individual amplitudes of production on N atoms [6], calculation of the square of the module amplitude and summing over all phonon states of the crystal. As a result, we obtain the coherent $\mathrm{d}\sigma_{\mathrm{coh}}(A_{2e})$ and incoherent contributions to the cross section in a crystal ($\hbar = c = 1$):

$$\frac{\mathrm{d}\sigma_{\mathrm{coh}}(A_{2e})}{\mathrm{d}\Omega} = \exp(-q^2\bar{u}^2)\left|\sum_{n=1}^{N} \exp(iq_{\parallel}nd)\right|^2 |S(q_{\parallel})|^2 \frac{\mathrm{d}\sigma_1(A_{2e})}{\mathrm{d}\Omega}, \tag{1}$$

$$\frac{\mathrm{d}\sigma_{\mathrm{incoh}}(A_{2e})}{\mathrm{d}\Omega} = N\left[1 - \exp(-q^2\bar{u}^2)\right]\frac{\mathrm{d}\sigma_1(A_{2e})}{\mathrm{d}\Omega}, \tag{2}$$

where $q^2 = \omega^2(1 + \beta^2 - 2\beta \cos \vartheta)$ is the transfered momentum squared and $q_{\parallel} = \omega(1 - \beta \cos \vartheta)$ is the parallel to the axis component of momentum transfered, ϑ is A_{2e} emission angle, $\bar{u}^2$ is the root-mean-square deviation of atoms from the equilibrium positions, d is the lattice constant, and $S(q_{\parallel})$ is the structure factor. The appearance of interferential multiplier

$$I_N = \left|\sum_{n=1}^{N} \exp(iq_{\parallel}nd)\right|^2$$

in Eq. (2) leads to the quantization of the longitudinal momentum transfer $q_{\parallel}$, and it follows that the cross-section has the sharp peaks at the photon energies defined by [12]:

$$\omega_n = \left(4m^2 + g_n^2\right)/2g_n, \qquad n = 1, 2, 3\ldots, \tag{3}$$

Fig. 1 shows sharp and large peaks for the ratio

$$R = \frac{\mathrm{d}\sigma_{\mathrm{coh}}(A_{2e}) + \mathrm{d}\sigma_{\mathrm{incoh}}(A_{2e})}{N\,\mathrm{d}\sigma_1(A_{2e})},$$

of the differential cross-section of coherent photoproduction of A_{2e} on a separate crystal string consisting of N atoms, to the differential cross-section on N atoms in an amorphous target, with taking into account the energy spread of the initial photon beam, $\Delta\omega/\omega = 10^{-2}$. The emission angle of positronium is taken $\vartheta_{A_{2e}} = \lambda/2\gamma_{A_{2e}}R_0$, i.e. $\vartheta_{A_{2e}}$ equals the angle for which the cross-section

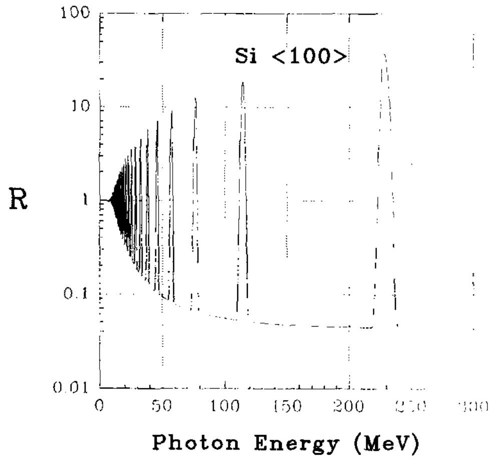

Fig. 1. The relation of the differential cross-sections of photoproduction of positronium atom (bound e^+e^- pair) on the crystal axis consisting of N atoms (Si⟨100⟩, $N = 10^3$, $T = 273$ K) to the same cross-section on N atoms in an amorphous target. The energy spread of incident photon beam $\Delta\omega/\omega = 10^{-2}$ is taken into account.

$\mathrm{d}\sigma_{\mathrm{coh}}(A_{2e})$ is maximal for given photon energy. Further, the calculations show that the quantity

$$R(\Delta_{A_{2e}}) = \frac{\int_0^{2\pi}\int_0^{\Delta_{A_{2e}}}[\mathrm{d}\sigma_{\mathrm{coh}}(A_{2e}) + \mathrm{d}\sigma_{\mathrm{incoh}}(A_{2e})] \sin\vartheta\,\mathrm{d}\vartheta\,\mathrm{d}\varphi}{N\int_0^{2\pi}\int_0^{\Delta_{A_{2e}}}\mathrm{d}\sigma_1(A_{2e}) \sin\vartheta\,\mathrm{d}\vartheta\,\mathrm{d}\varphi}, \tag{4}$$

which characterizes the increase of the yield in comparison with an amorphous target, as a function of the angular size $\Delta_{A_{2e}}$ of the detector, drops from $R(\Delta_{A_{2e}}) = 34$ at $\Delta_{A_{2e}} = 10^{-4}$ to $R(\Delta_{A_{2e}}) = 17$ at $\Delta_{A_{2e}} = 1 \times 10^{-3}$ and approaches $R(\Delta_{A_{2e}}) = 13.7$ at $\Delta_{A_{2e}} \to \pi$ (for the first coherent peak $n = 1$). For the photon energy $\omega \simeq 229$ MeV, near the first coherent peak, the total cross-section of coherent positronium photoproduction equals $\sigma_{\mathrm{cryst}} = \sigma_{\mathrm{coh}}(A_{2e}) + \sigma_{\mathrm{incoh}}(A_{2e}) \simeq 8.7$ mb (Si⟨100⟩, $N = 10^3$, $T = 273$ K). The value of $N = 10^3$ is chosen here taking into account the A_{2e} break-up during its passage through the target, as was discussed in Refs. [1,2,4].

3. Coherent pair production with K-shell capture by relativistic heavy ions in a crystal

3.1. Pair photoproduction with e^- K-shell capture in the Coulomb field

Now let us consider the pair production with e^- capture on K-shell under passage of fully stripped RHI through aligned crystal. We shall use below in Section 3.2 the virtual photon method and therefore here we start our calculation with evaluation of a simple formula for the cross-section of pair production by photon in the Coulomb field, with e^- capture into the K-shell. In the first Born approximation (the wave function of the positron is the plane wave and the wave function of electron is the wave function of a bound state) one has ($\hbar = c = 1$):

$$d\sigma_1 = 2\pi \left| e\sqrt{4\pi}\frac{1}{\sqrt{\omega}} M_{fi} \right| \delta(\varepsilon_+ + \varepsilon_- - \omega)\, d\nu, \tag{5}$$

where $\varepsilon_- \simeq m - \varepsilon_k$ and ε_+ are the energies of e^- and e^+, $\varepsilon_k = m(Z_{ion}e^2)^2/2$ is the energy of a bound state on K-shell, Z_{ion} is the target nucleus charge and

$$M_{fi} = \int \overline{\Psi}_f(e_\mu \gamma^\mu) e^{-ikr} \Psi_i \, d^3x \tag{6}$$

is the matrix element, $\boldsymbol{k}$ and ω are the energy and momentum of the photon, $d\nu = d^3\boldsymbol{p}_+/(2\pi)^3$ is a phase volume. Here, $\Psi_f = (u/\sqrt{2\varepsilon_-})\Phi$ is the wave function of bound state, with $\Phi = Ce^{-\eta r}$ being the nonrelativistic wave function of the bound state, u is the free electron Dirac spinor and $\eta = 1/a_0 = mZ_{ion}e^2$, $a_0 = Z_{ion}e^2/2\varepsilon_k$, $C = 1/\sqrt{\pi a_0^3}$; $\Psi_i = (u_1/\sqrt{2\varepsilon_-})e^{-ip_+r}$ is e^+ plane wave function with momentum $\boldsymbol{p}_+$, and u_1 is the free positron Dirac spinor. After substitution of these functions into (6) and standard calculations we arrive at

$$d\sigma_1 = \frac{Z_{ion}^2 e^2}{2\pi\omega}\frac{\varepsilon_+\varepsilon_- + m^2}{\varepsilon_+\varepsilon_-}\left[\frac{8\pi\eta C}{\left(\eta^2 + (\boldsymbol{k} - \boldsymbol{p}_+)^2\right)^2}\right]^2 \times \delta(\varepsilon_+ + \varepsilon_- - \omega)\, d^3\boldsymbol{p}_+. \tag{7}$$

The integration of Eq. (7) over positron momentum $d^3\boldsymbol{p}_+$ gives the total cross-section of the process:

$$\sigma_1(\omega) = \frac{32\pi}{3} e^2 a_0^{-5} \frac{[\varepsilon_+\varepsilon_- + m^2]}{\omega^2 \varepsilon_+} \times \left[\frac{(a+b)^3 - (a-b)^3}{(a^2 - b^2)^3}\right], \tag{8}$$

$$a + b = \eta^2 + (\omega + p)^2, \quad a - b = \eta^2 - (\omega + p)^2.$$

Fig. 2 presents the results of numerical calculation according to Eq. (8) of the total cross-section of e^+e^- pair photoproduction, with electron K-shell capture, on Pb^{82+}, upon the photon energy ω. From Fig. 2 follows that the cross-section has a broad maximum, the width of which is about 10 MeV.

In the high energy limit, $\omega \gg m$, $\varepsilon_+ \simeq \omega$ and for $Ze^2 \ll 1$ we obtain for the total cross section of pair photoproduction with electron K-shell capture more simple expression:

$$\sigma_{ph}(\omega) = \frac{32}{3}\pi e^2 a_0^{-5} m^{-6}\frac{1}{\omega},$$

which differs only by numerical constant from more exact results of papers [7–10] obtained in more sophisticated way with the use of the exact Dirac wave functions of outgoing e^+ and bound e^- in the Coulomb field. In fact, our simple model satisfactorily describes the shape of the cross-section, although overestimates the absolute value of the cross section, in comparison with, e.g. Ref. [10], Fig. 1.

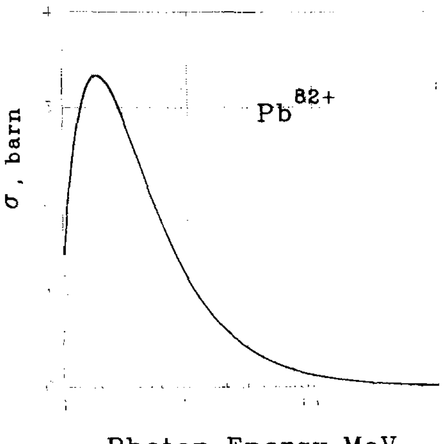

Fig. 2. The total photoproduction cross-section of e^+e^- pair with e^- K-shell-capture on Pb^{82+} is given as a function of the photon energy.

3.2. Coherent pair photoproduction with e^- K-shell capture under RHI passage through aligned crystal

The cross-section of e^+e^- production with electron K-shell capture by RHI, travelling parallel to the crystal axis, can be obtained by virtual photon (VP) method:

$$\frac{d\sigma}{d^3\boldsymbol{p}_+} = \int \frac{d\sigma_{ph}}{d^3\boldsymbol{p}_+} n(\omega)\, d\omega, \tag{9}$$

where $n(\omega)$ is the VP spectrum in the rest frame (RF) of the RHI, integrated over impact parameters and averaged over thermal vibrations of atoms in a crystal string. After substitution of Eq. (7) into (9) and integration over ω one has:

$$\frac{d\sigma}{d^3\boldsymbol{p}_+} = \frac{d\sigma_{ph}(\varepsilon_+ + \varepsilon_-)}{d^3\boldsymbol{p}_+} \times n(\varepsilon_+ + \varepsilon_-). \tag{10}$$

To derive the VP spectrum for the case when RHI moves along the crystal string, we followed Ter-Mikaelian [6] and obtained

$$n(k_1) = \int_{-\infty}^{\infty} \frac{k_\perp^2}{k_1\left(k_1^2 + k_\perp^2 + R^{-2}\right)^2} \left| \sum_{n=1}^{N} \exp(i\boldsymbol{k}_1 \boldsymbol{r}_n) \right|^2. \tag{11}$$

Here, the screened Coulomb potential $V(r) = (Ze/r) \times \exp(-r/R)$ of the crystal atom has been used, and $\boldsymbol{r}_n$ are the positions of atoms in the string. The last equation should be averaged over thermal vibrations of atoms in a crystal string. Since the dependence on the crystal variables consists only of the term $|\sum_{n=1}^{N} \exp(ik_{\perp}r_n)|^2$, the standard procedure of averaging [6] results in:

$$\overline{|\sum_{n=1}^{N} \exp(ik_{\perp}r_n)|^2} = N(1-\exp[-k^2\bar{u}^2]) + \exp[-k^2\bar{u}^2]\left|\sum_{n=1}^{N}\exp[ikr_{0n}]\right|^2 |S|^2, \quad (12)$$

where $k_{\parallel}r_{0n} = n\omega d/\gamma$, $r_{0n} = nd$ are equilibrium positions of atoms of the crystal axis, γ is the relativistic factor of RHI, ω is an energy of the VP, d is the lattice constant, S is the structure factor of a crystal axis and N is the number of atoms in a string. Therefore, the integration of Eq. (11) over $\mathrm{d}k_{\perp}$ results in

$$n(\omega)\,\mathrm{d}\omega = \frac{Z^2e^2}{\pi^2}\left\{N[L-BE] + BE\left|\sum_{n=1}^{N}\exp\left[i\frac{n\omega d}{\gamma}\right]\right|^2 |S|^2\right\}\frac{\mathrm{d}\omega}{\omega}. \quad (13)$$

The functions $B(\omega)$, $E(\omega)$ and $L(\omega)$ are defined as:

$$B(x) = \pi\{-(1+x)\,\mathrm{e}^{x}Ei(-x) - 1\},$$
$$x = \left[\frac{\omega^2}{\gamma^2} + R^{-2}\right]\bar{u}^2, \quad (14)$$

where $-Ei(-x)$ is the integral exponential function.

$$E(\omega) = \exp\left[-\frac{\omega^2\bar{u}^2}{\gamma^2}\right],$$
$$L(\omega) = \pi\ \ln\left[\frac{am^2}{\omega^2/\gamma^2 + R^{-2}}\right], \quad a \sim 1, \quad (15)$$

and $\bar{u}^2$ is the root mean-square deviation of atoms from the equilibrium positions.

The sum of exponents in Eq. (13) is again the interference multiplier as in Section 2.2, which takes into account the coherent effect, connected with periodic arrangement of the atoms in a string. It can be rewritten in a form:

$$I_N \equiv |\sum_{n=1}^{N}\exp[ikr_{0n}]|^2 = |\sum_{n=1}^{N}\exp(i\omega dn/\gamma)|^2 = \frac{\sin^2(N\omega\,\mathrm{d}/2\gamma)}{\sin^2(\omega\,\mathrm{d}/2\gamma)}, \quad (16)$$

from which immediately follows, that the interference multiplier has very sharp peaks equal to N^2 at

$$\omega d/2\gamma = \pi k, \qquad k = 1, 2, 3\ldots. \quad (17)$$

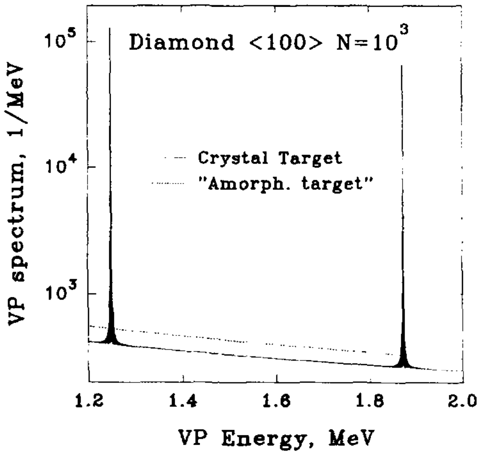

Fig. 3. The VP spectra $n(\omega)$ as it seen in the rest frame of the 170 GeV/u RHI: in ⟨100⟩ diamond crystal and in the case of $N = 10^3$ individual C atoms ("amorphous target"). The VP spectra are plotted as a function of VP energy. The solid curve is for the crystal target and the dashed curve is for "amorphous target". The width of every coherent peak is of order of $\omega_{\parallel}/N$, where $\omega_{\parallel} = 2\pi\gamma\beta/d$.

This is the reason, which leads to specific (peaked) shape of VP spectrum, see Fig. 3, which differs very much from ordinary VP spectrum in an amorphous target.

Using the invariance of the total cross-section in the rest frame (RF) (σ_{RF}) and in the laboratory frame (LF) (σ_{LF}), $\sigma_{LF} = \sigma_{RF}$ and the relativistic invariant $\mathrm{d}^3p_+/E = \mathrm{d}^3_{\mathrm{L}}p_+/E_{\mathrm{L}}$, one can transform the differential cross section from RF to LF. After the transformation of the Eq. (10) to the LS and some algebra, we find

$$\frac{\mathrm{d}\sigma_{LF}}{\mathrm{d}\varepsilon_+^{\mathrm{L}}\mathrm{d}\Omega_{\mathrm{L}}} = 32e^2a_0^{-5} \times \frac{\varepsilon_+\varepsilon_- + m^2}{\omega^*\varepsilon_+\varepsilon_-\left[\eta^2 + (\omega^*)^2 + p_+^2 + 2\omega^*p_{+\parallel}\right]^4} \times \frac{(\varepsilon_+^{\mathrm{L}})^2 p_+^{\mathrm{L}}}{\varepsilon_+}n(\omega^*); \quad (18)$$

here $\omega^* = \varepsilon_+ + \varepsilon_-$; $\varepsilon_+^{\mathrm{L}}$ and p_+^{L} are positron energy and momentum in LF; ε_+, p_+ and $p_{+\parallel}$ are positron energy, momentum and momentum component parallel to crystal string in RF which must be expressed through $\varepsilon_+^{\mathrm{L}}$ and p_+^{L} according to the Lorentz transformation rules. The further calculation has been done numerically.

Fig. 4 shows the differential over positron energy $\varepsilon_+^{\mathrm{L}}$ and emission solid angle cross-sections (18) of coherent e^+e^- pair production with e^- K-shell capture, under the penetration of relativistic Pb^{82+} ion ($E = 170$ GeV/u) through the ⟨100⟩ diamond crystal. Here, the positron emission angle is taken $\theta = 0.001$ rad. Fig. 4a presents the

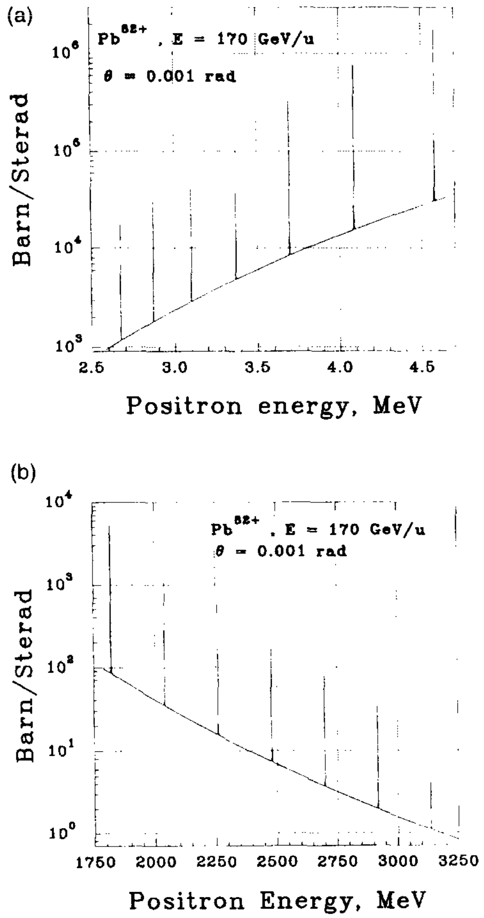

Fig. 4. The differential over positron energy cross section of coherent e^+e^- pair production with e^- K-shell capture by relativistic Pb^{82+} ($E = 170$ GeV/u) in ⟨100⟩ diamond crystal is shown as a function of emitted positron energy. The positron emission angle is $\theta = 0.001$ rad. (a) Presents the low-energy and (b) the high-energy parts of the cross-section, respectively.

low energy and 4b – the high energy parts of the cross-section.

As in the case of coherent A_{2e} photoproduction (Section 2.2), the sharp maxima arise (due to interferential multiplier (16)) in the differential over positron energy cross-section (Fig. 4a–b). The physical reason for appearance of coherent maxima is connected with sharp peaks in the VP spectrum in a crystal, see Fig. 3. Our calculations show that the relation of the coherent peaks to the incoherent background is rather high, of order of $10-10^2$.

It should be mentioned, that our simple consideration is only to call attention to the possible new effect in e^+e^- production by RHI in a crystal. Many factors, like the energy (angular) spread of initial RHI beam, bending of RHI trajectories in a crystal, the finite angular (energy) resolution of positron detectors can change the width and height of coherent peaks.

4. Conclusions

New possible coherent effects arising during interaction of high energy photons and RHI with a crystal have been considered. The physical reason for an appearance of brilliant coherent effects is connected here with well defined initial and final states in both processes, and with appearance of sharp peaks in the interference multiplier.

Indeed, for the case of photoproduction of relativistic positronium, if the emission angle of relativistic positronium atom is defined, the coherent peaks appear only at definite photon energy, since the positronium energy is exactly defined by photon energy and binding energy in a positronium. Therefore, the coherent peaks for the case of photoproduction of relativistic positronium in a crystal are much more brilliant in comparison with those for coherent photoproduction of free electron–positron pairs (even well collimated) in a crystal, (see, e.g., Ref. [11]) where it was shown, that under detection of pairs with restricted emission angles the coherent peaks become more brilliant in comparison with total (integrated over all emission angles) cross-section of coherent pair photoproduction.

The coherent positronium production by relativistic electrons was first considered by Sandnes and Olsen [12], where it was shown, that the interesting coherent effects appear both for triplet and for singlet positronia electroproduction.

For the case of coherent pair creation by RHI with electron K-shell capture, the interferential multiplyer (in the RF) has sharp peaks when both RHI energy and positron energy are fixed; therefore in LF the emitted positron spectrum has sharp maxima, the positions of which depend on the positron emission angle. For comparison, no peculiarities in energy (angular) spectra of emitted positrons exist for this process in an amorphous target, since the VP spectrum in this case is continuous and does not contain the sharp peaks as in the case of a crystal.

The coherent effect for pair production with K-shell capture by other relativistic heavy particles one can calculate in a similar way as we have considered here for the case of RHI passing through the crystal. The interesting partial case could be the coherent creation of the antihydrogen atom by relativistic antiproton channeled in a crystal, as recently considered in [13].

The structures presented in the calculations could not be an artificial effect of the present simple models; the structures are the consequence of the periodicity of arrangement of atoms in the string and will persist even if one utilizes the relativistic dynamics (exact Dirac wave functions). Similar structures are well known for coherent bremsstrahlung and coherent pair production [6,11], for coherent excitation of fast hydrogen-like ions [14] in the crystals.

Both considered processes can be studied experimentally using monochromatic (or tagged) 10^2-10^3 MeV photon beams and 10^2-10^3 GeV/nucleon RHI beams.

Acknowledgement

The authors are grateful to V.M. Strakhovenko for useful discussion.

References

[1] Yu.P. Kunashenko and Yu.L. Pivovarov, Yad. Fiz. 51 (1990) 627 [Sov. J. Nucl. Phys. 51 (3) (1990) 397].
[2] Yu.P. Kunashenko and Yu.L. Pivovarov, Izv. Akad. Nauk. Ser. Fiz. 57 (1993) 156 (Bull. Russ. Acad. Sci. Phys. 57 (1993) 144].
[3] Yu.P. Kunashenko and Yu.L. Pivovarov, Book of Abstracts in: Workshop on Channeling and Other Coherent Effects of Relativistic Energy (University of Aarhus, July 10–14, 1995) p. 37.
[4] H.A. Olsen, Phys. Rev. D 33 (1986) 2033.
[5] V.L. Luboshits Yad. Fiz. 45 (1987) 1099 [Sov. J. Nucl. Phys. 45 (1987) 682].
[6] M.L. Ter-Mikaelian, High-Energy Electromagnetic Processes in Condensed Media (Wiley–Interscience, New York, 1972).
[7] C.A. Bertulani and G. Baur, Phys. Rep. 163 (1988) 299.
[8] A.I. Milstein and V.M. Strakhovenko, JETP 76 (1993) 775 (Zh. Eksp. Teor. Fiz. 103 (1993)).
[9] G. Baur, Phys. Lett. B 311 (1993) 343.
[10] A. Aste, K. Henchken, D. Trautmann and G. Baur, Phys. Rev. A 50 (1994) 3980.
[11] Yu.P. Kunashenko and Yu.L. Pivovarov, Nucl. Instr. and Meth. B 114 (1996) 237.
[12] G.I. Sandnes and H.A. Olsen, Phys. Rev. A 48 (1993) 3725.
[13] Yu.P. Kunashenko, O.E. Krivosheev and Yu.L. Pivovarov, Book of Abstracts in XXV Intern. Conf. Physics of Interactions of Fast Charged Particles with Crystals (Moscow Univ. Pub. House, Moscow, 1995) p. 25.
[14] S. Datz and C.D. Moak, in: Treatise on Heavy-Ion Science, Vol. 6, ed. D.A. Bromley (Plenum, New York, 1985).